

Determination of the Resonant Frequencies in a Complex Cavity Using the Scattering Matrix Formulation

JEFF M. NEILSON, MEMBER, IEEE, PETER E. LATHAM, MEMBER, IEEE, MALCOLM CAPLAN,
AND WESLEY G. LAWSON, MEMBER, IEEE

Abstract — A method for computing the resonant frequency in a complex cavity consisting of a series of waveguide sections is derived. The analysis uses the scattering matrix formulation to produce an eigenvalue equation which must be solved numerically. The technique is easily implemented numerically and shows good agreement with experiment.

I. INTRODUCTION

FINDING the resonant frequencies and Q values in a complex cavity is a problem of practical importance in many applications. While finite mesh codes can be used in the general case, there is a class of geometries that admits a much simpler and faster solution. Namely, when the cavity consists of a series of waveguide sections, the scattering matrix method [1]–[6] may be applied. Such a configuration is shown in Fig. 1(a). The ends may be open or closed and the waveguide shape may change from one section to the next (e.g., circular to square to rectangular).

Our analysis is restricted to transitions in which one waveguide is wholly contained in the other; “mixed” boundary conditions such as the one illustrated in Fig. 1(b) may be handled by placing a zero-length section of waveguide in the overlap region [2]. We also require that the waveguide sidewalls be parallel to each other and perpendicular to the end walls. Tapered sections can be modeled as a series of small transitions. For simplicity we assume that all surfaces are perfectly conducting and that the cavity is filled with a material of a uniform dielectric constant ϵ and permittivity μ , although the formalism applies to more complex configurations.

An eigenvalue problem is formed by cascading the scattering matrix from a given section outwards to the ends of the complex cavity, with appropriate boundary conditions at the ends. The eigenvalue equation is solved numerically by searching for a complex frequency, the cavity Q being determined by half of the ratio of the real to the imaginary

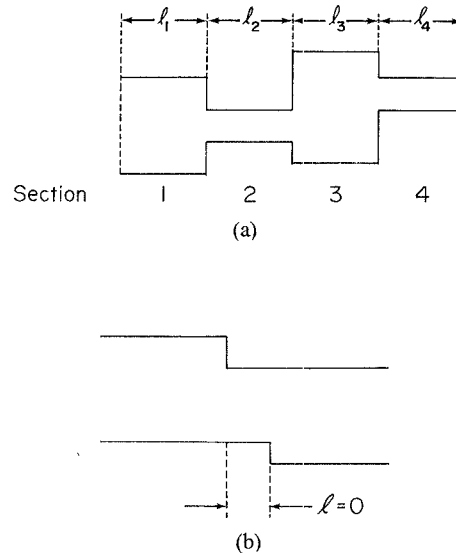


Fig. 1. (a) A typical complex cavity. Each section has a uniform cross section and length l^i . The ends may be closed or open; in the latter case we consider either l^1 or l^4 going to infinity or provide perfect terminations. (b) “Mixed” boundary conditions are incorporated into our analysis by inserting a zero section of waveguide in the region of overlap.

part of the frequency. Alternatively, one may solve the eigenvalue equation with the frequency and Q fixed by varying the cavity dimensions. If both ends of the cavity are closed and ϵ and μ are real, only a one-dimensional search for the real part of the frequency need be performed.

In Section II we derive the formalism used to determine the resonant frequencies and Q values of a given cavity, and in Section III we show results obtained from a code based on the formalism. Section IV contains our summary and conclusions.

II. FORMALISM

Calculation of the scattering matrices is implemented by the mode-matching technique. Details of the derivation can be found in numerous papers [1]–[6], so we shall only briefly outline the development here. The derivation begins by assuming an expansion of the transverse fields E and

Manuscript received August 15, 1988; revised April 11, 1989.
J. M. Neilson is with Varian Associates, 611 Hansen Way, Palo Alto, CA 94303.

P. E. Latham and W. G. Lawson are with the Laboratory for Plasma Research, University of Maryland, College Park, MD 20742.

M. Caplan was with Varian Associates, Palo Alto, CA. He is now with the Lawrence Livermore National Laboratory, University of California, Livermore, CA 94550.

IEEE Log Number 8928843.

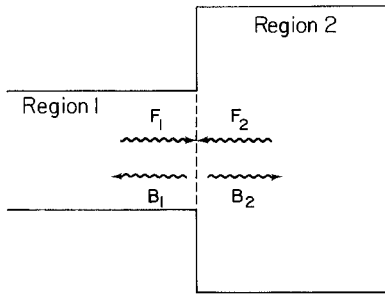


Fig. 2. Definition of mode amplitudes in scattering matrix formulation.

H in terms of the eigenmodes \vec{e}_i, \vec{h}_i of the waveguide in region 1 as

$$\vec{E}_1 = \sum_{i=1}^M (F_{i1} + B_{i1}) \vec{e}_i \quad (1a)$$

$$\vec{H}_1 = \sum_{i=1}^M \left(\frac{F_{i1} - B_{i1}}{Z_{i1}} \right) \vec{h}_i \quad (1b)$$

where F is the modal amplitude of the forward (propagating in the $+z$ direction) wave, B is the amplitude of the backward wave, and Z is the characteristic impedance (see eq. (A6) of the Appendix). The fields in the second region are defined similarly, being

$$\vec{E}_2 = \sum_{j=1}^N (F_{j2} + B_{j2}) \vec{e}_j \quad (2a)$$

$$\vec{H}_2 = \sum_{j=1}^N \left(\frac{F_{j2} - B_{j2}}{Z_{j2}} \right) \vec{h}_j. \quad (2b)$$

The value of N is governed by the relative convergence phenomenon [7], [8] and for circular waveguides is given by the radii ratio times the value of M .

Applying continuity of tangential E and H across the common aperture area and enforcing zero tangential electric field on the wall of the larger guide yields the following relation between the forward and backward mode amplitudes in the guides:

$$P[\underline{F}_1 + \underline{B}_1] = I[\underline{F}_2 + \underline{B}_2] \quad (3a)$$

$$Z_1 P^T Y_2 [\underline{F}_2 - \underline{B}_2] = I[\underline{F}_1 - \underline{B}_1] \quad (3b)$$

where I is the identity matrix; \underline{F} and \underline{B} are vectors containing the unknown mode amplitude coefficients ($F_{1l} \dots F_{Kl}$, $B_{1l} \dots B_{Kl}$) for regions $l=1,2$; Z_1 is an $N \times N$ diagonal matrix of the modal impedances in region 1; and Y_2 is an $M \times M$ diagonal matrix of the modal admittances for region 2 ($Y_2 = Z_2^{-1}$). The elements of the mode coupling matrix P are given by

$$P_{jl} = \int_{CA} \vec{e}_{j2} \cdot \vec{e}_{i1}^* dA \quad (4)$$

where the integration is performed over the common aperture area between the guides, and the normalization is chosen so that $\int \vec{e}_j \cdot \vec{e}_j^* dA = 1$ and $\vec{h}_i = \hat{z} \times \vec{e}_i$.

The voltage scattering matrix formulation (Fig. 2) for the forward and backward waves is defined as

$$\underline{B} = S \underline{F} \quad (5)$$

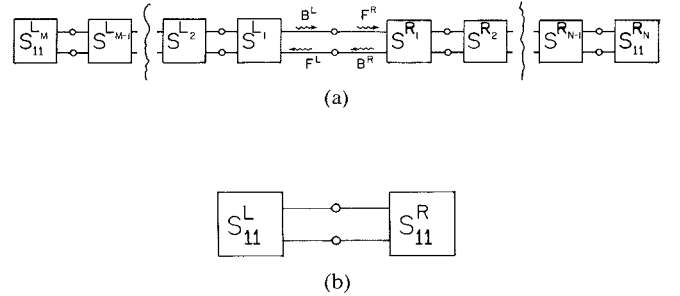


Fig. 3. Cascading matrices: (a) original problem; (b) result from cascading matrices to left and right.

where

$$\underline{B} = \begin{pmatrix} B_1 \\ B_2 \end{pmatrix} \quad \underline{F} = \begin{pmatrix} F_1 \\ F_2 \end{pmatrix} \quad S = \begin{pmatrix} S_{11} & S_{12} \\ S_{21} & S_{22} \end{pmatrix}.$$

Rearranging (3) into the scattering matrix formulation yields

$$S_{11} = [I + Z_1 P^T Y_2 P]^{-1} [I - Z_1 P^T Y_2 P] \quad (6a)$$

$$S_{12} = 2[I + Z_1 P^T Y_2 P]^{-1} Z_1 P^T Y_2 \quad (6b)$$

$$S_{21} = 2[I + P Z_1 P^T Y_2]^{-1} P \quad (6c)$$

$$S_{22} = -[I + P Z_1 P^T Y_2]^{-1} [I - P Z_1 P^T Y_2]. \quad (6d)$$

To determine the resonant frequency for a given configuration, the scattering matrices are cascaded from the cavity section outwards to the left and right (Fig. 3). The boundary conditions at the ends determine the final scattering matrix. For matched waveguide sections, $S_{11} = 0$, while for shorted sections $S_{11} = -I$.

Cascading [3] the scattering matrices from both the left and the right into the cavity section leads to the set of equations

$$\underline{B}^R = S_{11}^R \underline{F}^R \quad (7a)$$

$$\underline{B}^L = S_{11}^L \underline{F}^L \quad (7b)$$

where S_{11}^L resulted from cascading the scattering matrices from the cavity section to the left and S_{11}^R is the scattering matrix for the cascaded scattering matrices to the right. Combining (7a) and (7b) results in the matrix equation

$$\underline{B}^R = S_{11}^R S_{11}^L \underline{B}^R \quad (8)$$

so that

$$\det(S_{11}^R S_{11}^L - I) = 0. \quad (9)$$

The amplitude of the backward mode in the cavity section is the eigenvector of $S_{11}^L S_{11}^R$ with eigenvalue 1, and $\underline{F}^R = S_{11}^L \underline{B}^R$. Once \underline{F}^R and \underline{B}^R have been determined, the amplitudes of the forward and backward waves in all sections may be found by back-cascading the scattering matrices. For scattering from a smaller to a larger waveguide (see Fig. 4), the amplitude of the forward mode in the $k+1$ (larger) section is obtained from (3a) and is

$$F_{k+1} = (I + S_{11}^{R'})^{-1} P(F'_k + \underline{B}_k) \quad (10)$$

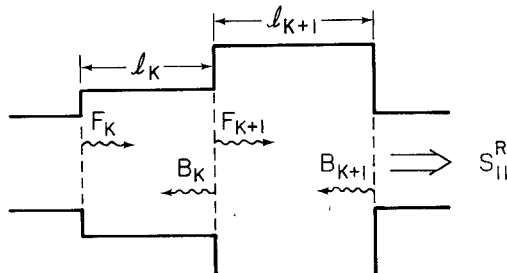


Fig. 4. Calculation of field amplitudes.

where the prime indicates a change in phase given by

$$S_{11}^R = I \cdot \exp(-\beta_{k+1} l_{k+1}) S_{11}^R I \cdot \exp(-\beta_{k+1} l_{k+1})$$

$$F'_k = I \cdot \exp(-\beta_k l_k) F_k$$

with β being a vector of the complex propagation constants of the modes. For scattering from a larger to a smaller waveguide the amplitude of the forward mode obtained from (3b) is given by

$$F_{k+1} = (I - S_{11}^R)^{-1} Z_{k+1} P^T Y_k (F'_k - B_k). \quad (11)$$

The algorithm for finding the resonant frequencies of a cylindrical cavity of arbitrary geometry modeled by a series of sudden transitions may be summarized as follows:

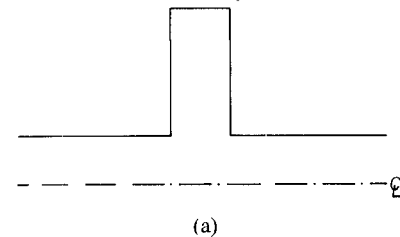
- 1) Construct the frequency-independent coupling matrices P_{μ} .
- 2) Calculate the scattering matrices at each transition and cascade them outward from the cavity section to form the left and the right scattering matrix.
- 3) Form the eigenvalue equation from the left and right scattering matrices.
- 4) Solve the eigenvalue equation (repeating steps 2 and 3) by a two-dimensional search in complex frequency or, for closed cavities and real dielectric constant and permittivity, a one-dimensional search in real frequency.

In practice, this method converges rapidly—generally in less than ten iterations. The results are insensitive to the section in which the eigenvalue equation is formed unless one of the sections is cut off at the frequency of interest. No spurious cavity resonances have been observed for cavities with finite Q values.

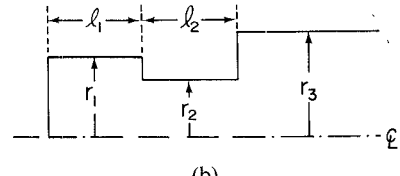
III. NUMERICAL RESULTS

Using this formalism a code was written to find the resonant frequencies and Q values in a system of cylindrical cavities. Configurations applicable to gyrotron amplifiers [9] and oscillators [10] were considered; these are shown in Figs. 5 and 9 respectively. Since all cavities have the same axis of symmetry, the coupling matrices may be found analytically and are given in the Appendix.

Transmission measurements were used to determine the frequency and Q of the complex cavities depicted in Fig. 5. The experimental setup is shown in Fig. 6. The mode converters were $TE_{10} \rightarrow TE_{11}$ nonresonant transitions for the buncher cavity and $TE_{10} \rightarrow TE_{01}$ Marie transitions for



(a)



(b)

Fig. 5. Cavities used in comparison of theory and experiment: (a) buncher cavity; (b) output cavity.

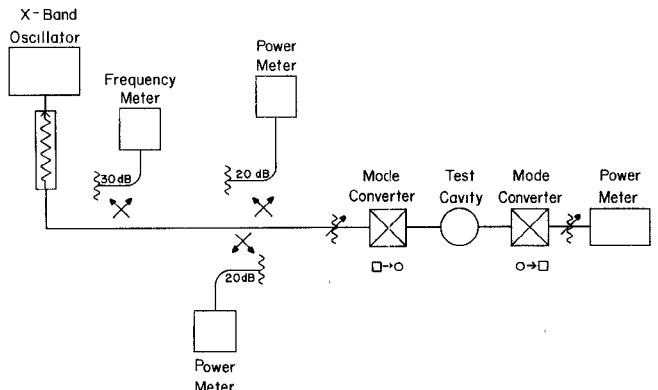
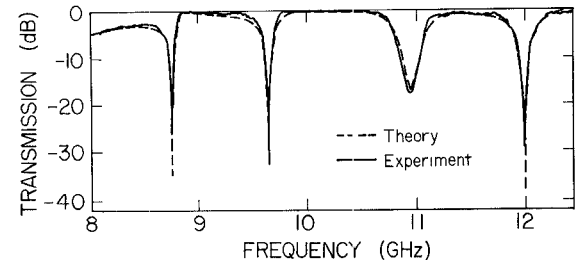
Fig. 6. Experimental setup for measurement of frequency and Q values of test cavities.

Fig. 7. Comparison between theory and experiment for transmission measurement of buncher cavities.

the output cavity. The buncher cavity had a 1.27 cm drift tube radius, a 4.5 cm cavity radius, and a 1.53 cm cavity length. The theoretical and experimental TE_{11} X -band transmission curves were in excellent agreement and are shown in Fig. 7. The output cavities incorporated a simple coupling iris to control the cavity Q and were designed using the code to have a Q of 300 with a TE_{01} cavity mode. The results of the calculation and measurements for the cavities are listed in Table I. They are in good agreement, with error in the Q calculation of less than 10 percent and calculated frequency errors less than 1 per-

TABLE I
COMPARISON OF THEORY AND EXPERIMENT FOR THE TE_{01} OUTPUT CAVITY

r_1	r_2	r_3	l_1	l_2	Experiment		Theory	
					f_o	Q	f_o	Q
2.109	1.500	2.700	2.700	0.468	9.99	295 ± 11	10.01	307
2.109	1.650	2.700	2.520	1.080	10.00	285 ± 10	10.00	307
2.109	1.800	2.700	2.109	2.667	9.98	325 ± 15	10.00	302

Lengths are in cm and frequencies in GHz. Twelve modes were used in the field expansion in section one.

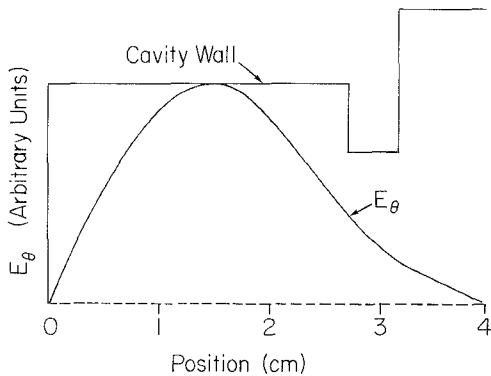


Fig. 8. Calculated mode profile for output cavity.

cent. The error estimates include only the effect of an additional coupling aperture required to inject the microwave signal. A plot of the mode profile for the first output cavity is shown in Fig. 8.

The frequency and Q converge rapidly as the number of modes used in the field expansion increases. Typically only 5–15 modes are required. We note that for calculation of field amplitudes near edges many more modes are required; however, for purposes of calculation of frequency and Q the inclusion of these modes results only in a significant increase in computation time with no increase in accuracy of the calculation.

The cavity shown in Fig. 9 uses both a linear taper and an iris to set cavity Q and mode profile. Table II shows the results for the calculation and measurement of the cavity. Ten steps were used to model the linear taper in the cavity section. The agreement between measurement and calculation is again good. The calculated mode profile is depicted in Fig. 10.

IV. SUMMARY

Using the scattering matrix formalism, we have developed a method for computing the resonant frequencies and Q values in a complex cavity consisting of a series of waveguides. This method is suitable for modeling both abrupt changes in radius and smoothly varying tapers. The formalism can easily be extended to model more commonly used cavities such as those found in klystrons and accelerators. It is easy to implement numerically, converges rapidly (many times faster than finite mesh codes),

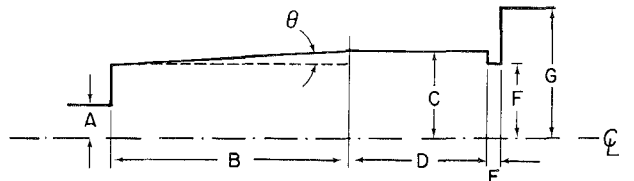


Fig. 9. Output cavity with linear taper.

TABLE II
COMPARISON OF THEORY AND EXPERIMENT FOR THE TE_{02} TAPERED CAVITY

A	B	C	D	E	F	G	Experiment		Theory	
							f_o	Q	f_o	Q
0.544	3.300	1.207	1.778	0.119	1.181	1.444	27.96	450	28.01	475

Lengths are in cm and frequencies in GHz. Taper angle was 0.48° and eight modes were used in the straight section of the cavity

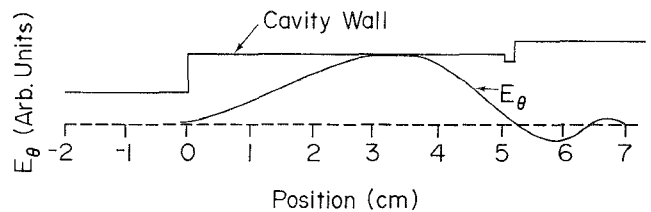


Fig. 10. Calculated mode profile for output cavity with linear taper

and is free of spurious solutions. Good agreement was found between theory and experiment.

APPENDIX EIGENMODES, WAVE IMPEDANCE, AND COUPLING EQUATION FOR CIRCULAR WAVEGUIDE

The following definitions of the eigenmodes and wave impedances were used in the cylindrical cavity code. MKS units are used in all equations. TE eigenmodes for the transverse electric fields are

$$\vec{e}_{mn} = \frac{\sqrt{\epsilon_m}}{\sqrt{\pi} J_m(\gamma'_{mn})(\gamma'_{mn}^2 - m^2)^{1/2}} \left[\frac{m}{r} J_m\left(\frac{\gamma'_{mn} r}{a}\right) \sin(m\theta) \hat{r} + \frac{\gamma'_{mn}}{a} J'_m\left(\frac{\gamma'_{mn} r}{a}\right) \cos(m\theta) \hat{\theta} \right] \quad (A1)$$

while the TM eigenmodes are

$$\vec{e}_{mn} = -\frac{\sqrt{2}}{\sqrt{\pi} \gamma_{mn} J_{m-1}(\gamma_{mn})} \left[\frac{\gamma_{mn}}{a} J'_m\left(\frac{\gamma_{mn} r}{a}\right) \sin(m\theta) \hat{r} + \frac{m}{r} J_m\left(\frac{\gamma_{mn} r}{a}\right) \cos(m\theta) \hat{\theta} \right] \quad (A2)$$

where γ_{mn} is the n th zero of J_m , γ'_{mn} is the n th zero of J'_m , a is the cavity radius, and ϵ_m is defined as

$$\epsilon_m = \begin{cases} 1, & m = 0 \\ 2, & m \neq 0 \end{cases} \quad (A3)$$

The transverse magnetic field is given by $\vec{h}_{mn} = \hat{z} \times \hat{e}_{mn}$. Normalization of the TE and TM modes was chosen so the modes are orthonormal, that is,

$$\int \vec{e}_{mn} \cdot \vec{e}_{m'n'}^* dA = \delta_{mm'} \delta_{nn'}. \quad (\text{A4})$$

The propagation constant and wave impedances are

$$\beta_{mn} = \left(\left(\frac{\gamma_{mn}}{a} \right)^2 - k^2 \right)^{1/2} \quad (\text{A5})$$

$$Z_{mn} = \begin{cases} \frac{j\omega\mu}{\beta_{mn}} & \text{TE} \\ \frac{-j\beta_{mn}}{\omega\epsilon} & \text{TM} \end{cases} \quad (\text{A6})$$

where $k^2 = \mu\epsilon\omega^2$. The coupling coefficients for a system in which all waveguides share the same axis of symmetry are as follows:

$\text{TE}_1 \rightarrow \text{TE}_2$,

$$P_{n_1 n_2} = \frac{2 \left(\frac{a_1}{a_2} \right) \gamma'_{n_2} J' \left(\gamma'_{n_2} \frac{a_1}{a_2} \right)}{J(\gamma'_{n_2}) (\gamma'^2_{n_1} - m^2)^{1/2} (\gamma'^2_{n_2} - m^2)^{1/2} \left(1 - \left(\frac{\gamma'_{n_2}}{\gamma'_{n_1}} \right)^2 \left(\frac{a_1}{a_2} \right)^2 \right)} \quad (\text{A7})$$

$\text{TE}_1 \rightarrow \text{TM}_2$,

$$P_{n_1 n_2} = - \frac{2mJ \left(\gamma'_{n_2} \frac{a_1}{a_2} \right)}{\gamma'_{n_2} J_{m+1}(\gamma'_{n_2}) (\gamma'^2_{n_1} - m^2)^{1/2}} \quad (\text{A8})$$

$\text{TM}_1 \rightarrow \text{TM}_2$,

$$P_{n_1 n_2} = - \frac{2J \left(\gamma'_{n_2} \frac{a_1}{a_2} \right)}{\gamma'_{n_2} J_{m+1}(\gamma'_{n_2}) \left(1 - \left(\frac{\gamma'_{n_1}}{\gamma'_{n_2}} \right)^2 \left(\frac{a_2}{a_1} \right)^2 \right)}. \quad (\text{A9})$$

There is no coupling from TM modes in the smaller guide to TE modes in the larger guide. The subscripts on a and n refer to the guide section, a_1 and n_1 being the radius and mode index of the smaller section. The subscript 2 applies to the larger section. Since for centered guides there is no azimuthal mode coupling, the subscript m was dropped where not needed in the coupling expressions.

REFERENCES

- [1] A. Wexler, "Solution of waveguide discontinuities by modal analysis," *IEEE Trans. Microwave Theory Tech.*, vol. MTT-15, p. 508, 1967.
- [2] R. Safavi-Naini and R. H. Macphie, "On solving waveguide junction scattering problems by the conservation of complex power technique," *IEEE Trans. Microwave Theory Tech.*, vol. MTT-29, p. 337, 1981.
- [3] C. L. James, "Analysis and design of TE_{11} -to- HE_{11} corrugated cylindrical waveguide mode converters," *IEEE Trans. Microwave Theory Tech.*, vol. MTT-29, p. 1059, 1981.
- [4] H. Patzelt and F. Arndt, "Double-plane steps in rectangular waveguides and their application for transformers, irises, and filters," *IEEE Trans. Microwave Theory Tech.*, vol. MTT-30, p. 771, 1982.
- [5] H. Auda and R. F. Harrington, "A moment solution for waveguide junction problems," *IEEE Trans. Microwave Theory Tech.*, vol. MTT-31, p. 515, 1983.
- [6] A. S. Omar and K. Schünemann, "Transmission matrix representation of finline discontinuity," *IEEE Trans. Microwave Theory Tech.*, vol. MTT-33, p. 765, 1985.
- [7] R. Mittra, "Relative convergence of the solution of a doubly infinite set of equations," *J. Res. Natl. Bur. Stand., Sect. D*, vol. 67D, p. 245 (1963).
- [8] R. Mittra, T. Itoh, and Ti-Shu Li, "Analytical and numerical studies of the relative convergence phenomenon arising in the solution of an integral equation by the moment method," *IEEE Trans. Microwave Theory Tech.*, vol. MTT-20, p. 96, 1972.
- [9] K. R. Chu, V. L. Granatstein, P. E. Latham, W. Lawson, and C. D. Striffler, "A 30-MW gyrokylystron-amplifier design for high-energy linear accelerators," *IEEE Trans. Plasma Sci.*, vol. PS-13, p. 424, 1985.
- [10] J. Shively *et al.*, "Development program for a 200 kW, CW, 28 GHz gyrokylystron," Final Report, Apr. 1976 through Sept. 1980, Varian Associates, Inc., D.O.E. Contract No. W-7405-eng-26.

✖

Jeff M. Neilson (M'86) received the B.S. degree in engineering from California Polytechnic University in 1982 and the M.E. and degree of electrical engineer from the University of Utah in 1983 and 1985 respectively.

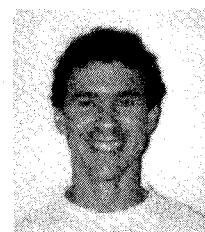
He has been employed at Varian Associates, Palo Alto, CA, for five years in the gyrotron department, where he has been involved in the analysis and design of high-power gyrotron tubes.

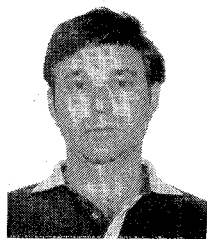


✖

Peter E. Latham (M'87) received the B.A. degree from the University of California at San Diego in 1977. He went on to the University of California at Berkeley, where he received the M.A. degree in physics in 1977 and the Ph.D. degree in physics in 1986.

Currently he is working on high-power microwave devices, including gyrotrons and free electron lasers, at the University of Maryland, College Park.





Malcolm Caplan received degrees in physics (with honors) and electrical engineering from the University of Alberta, Canada, and the Ph.D. degree in physics from U.C.L.A.

He worked at Hughes Aircraft Company and Varian Associates, Inc., Palo Alto, CA, from 1978 to 1986 developing gyrotron oscillators, gyrotron amplifiers, and gyrokylystrons. He is presently employed at Lawrence Livermore National Laboratory, Livermore, CA, in the development of high-power microwave source driver by induction linacs, in particular, CARMS, FEL's, and relativistic klystrons.



Wesley G. Lawson (S'84-M'85) was born in Akron, OH, in 1958. He received the B.S. degree in mathematics and the B.S., M.S., and Ph.D. degrees in electrical engineering from the University of Maryland.

He worked four years on electronics at Harry Diamond Laboratories and has worked seven years on microwave sources at the University of Maryland's Charged Particle Beam Laboratory, College Park, where he is currently an Assistant Professor.